File S1

SUPPORTING MATERIAL AND METHODS

DNA isolation and denaturing in-gel hybridization: Yeast genomic DNA was isolated using a Yeast DNA Extraction Kit (Thermo Scientific). The DNA was digested with XhoI restriction endonuclease before running on a 0.8% agarose gel. Denaturing in-gel hybridization using a telomeric CA oligonucleotide radio- labeled probe was performed as described (DIONNE and WELLINGER 1996)

Telospot: Telospot assays were performed as previously described (CRISTOFARI *et al.* 2007), except that the membrane was not denatured with NaOH. For Figure 6C, Telospot reactions were performed with 35 nM 5′-biotinylated $(TTAGGG)_3$ primer, which were then purified using 10 µl of streptavidin-coated M-280 Dynabeads (Invitrogen) according to the manufacturer's protocol. Samples were heated to 98°C for 5 min in 98% formamide-10 mM EDTA, resolved on a 12% polyacrylamide-urea gel, and transferred onto a positively charged Nylon membrane (GE Healthcare) using a semi-dry electrophoretic transfer cell (Transblot SD, BIO-RAD). After UV-crosslinking, the membrane was probed as in a standard Telospot assay.

SUPPORTING INFORMATION REGARDING THE VIABILITY OF *rnr1Δ*

To further examine the viability of an *rnr1Δ* deletion mutation in the BY4741 background, we backcrossed MCY602 (*rnr1Δ::kanMX* in the BY4741 background) to W9100-12C (a wild type strain of the W303 background). Half of the *rnr1Δ* progeny were dead (22 of 42 possible spores from 21 tetrad dissections), suggesting that one genetic locus was responsible for the difference in viability in the two genetic backgrounds.

Since Rnr3 protein levels are increased in *rnr1Δ* mutants (Figure 5), we wanted to determine if this single genetic locus was linked to *RNR3*. To do so, we crossed MCY605 (*rnr3Δ::natMX*; BY4742 background) and MCY606 (*yil067cΔ::natMX*; BY4742 background) to MCY602. *YIL067C* is adjacent to *RNR3* on chromosome IX. We were able to obtain viable *rnr1Δ yil067cΔ* double mutants, but not *rnr1Δ rnr3Δ* double mutants, indicating that Rnr3 is required for viability in the absence of Rnr1. We then crossed MCY607 (*rnr1Δ::kanMX yil067cΔ::natMX*; BY4741 background) to W9100-12C. As expected, half of the *rnr1Δ* progeny were dead (13 of 24 possible spores from 12 tetrad dissections). If the locus in question is linked to *RNR3*, then all the viable *rnr1Δ* strains should also contain *yil067cΔ::natMX* (of the 11 viable *rnr1Δ* colonies, only 8 were big enough to be genotyped by replica plating). This was not the case: only half did (5 of the 8). Thus, while a single genetic locus is responsible for the viability of *rnr1Δ* in the BY4741 background, the locus is not linked to *RNR3*.

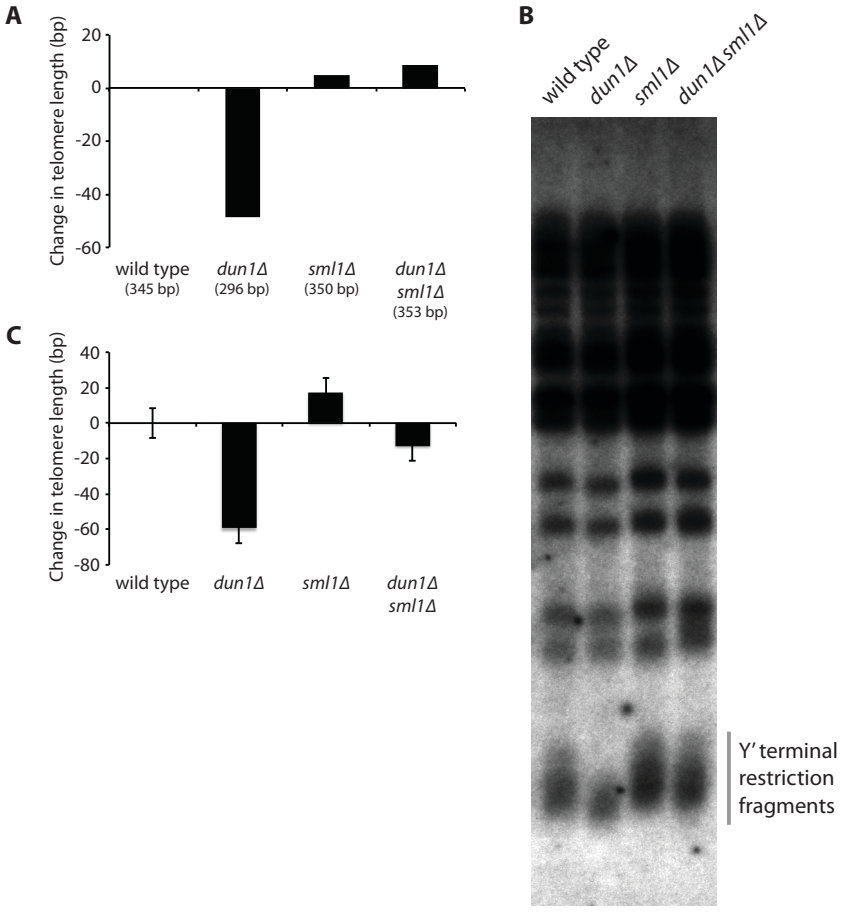

Figure S1. Telomeres are shortened in cells lacking Dun1. (A) Strains of the indicated genotypes were assayed for telomere length by telomere I-L PCR after being passaged for at least 100 generations. The change in telomere length, compared to wild type telomere length, was quantified and plotted. (B) Strains in A were assayed for telomere length by denaturing in-gel hybridization (see Supplementary Materials and Methods; a representative gel is shown). The vertical bar indicates the position of the terminal restriction fragments of Y′ telomeres, which represent more than half of yeast telomeres. Larger bands represent non-Y′-containing telomeres. (C) The change in telomere length, compared to wild type telomere length, of each strain indicated in B was quantified and plotted. Mean ± standard error for four independent isolates for each genotype are shown.

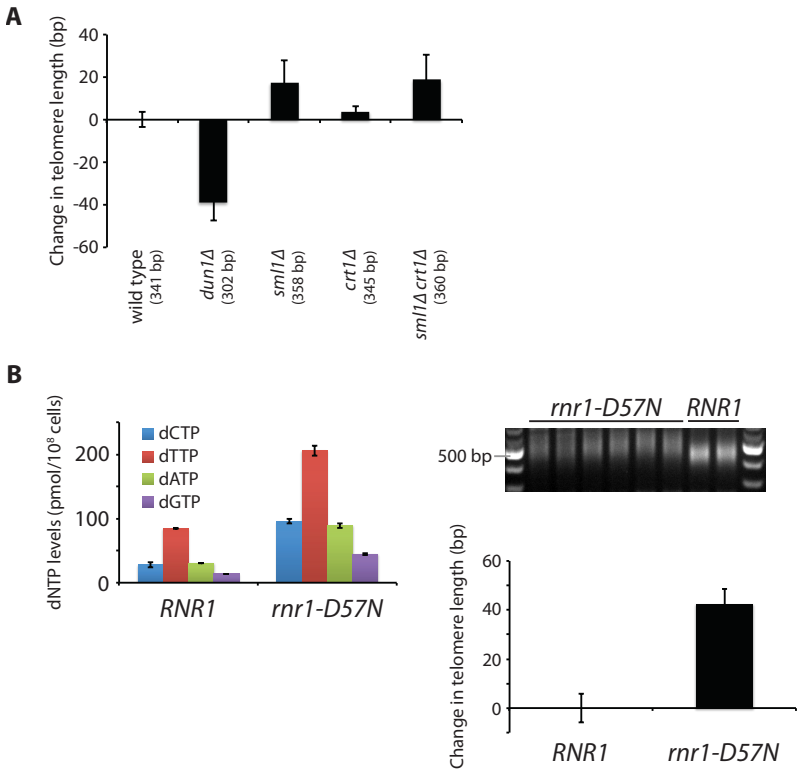

Figure S2. (A) The change in telomere length, compared to wild type telomere length, of strains of the indicated genotypes was quantified and plotted. Telomere length was assayed by Y′ telomere PCR. Mean ± standard error for at least three independent isolates for each genotype are shown. (B) Wild type (*RNR1*) and *rnr1-D57N* strains were assayed for dNTP levels. Data are represented as mean ± standard error. Multiple isolates of these strains were assayed for telomere length by Y′ telomere PCR (a representative gel is shown) and plotted as in A.

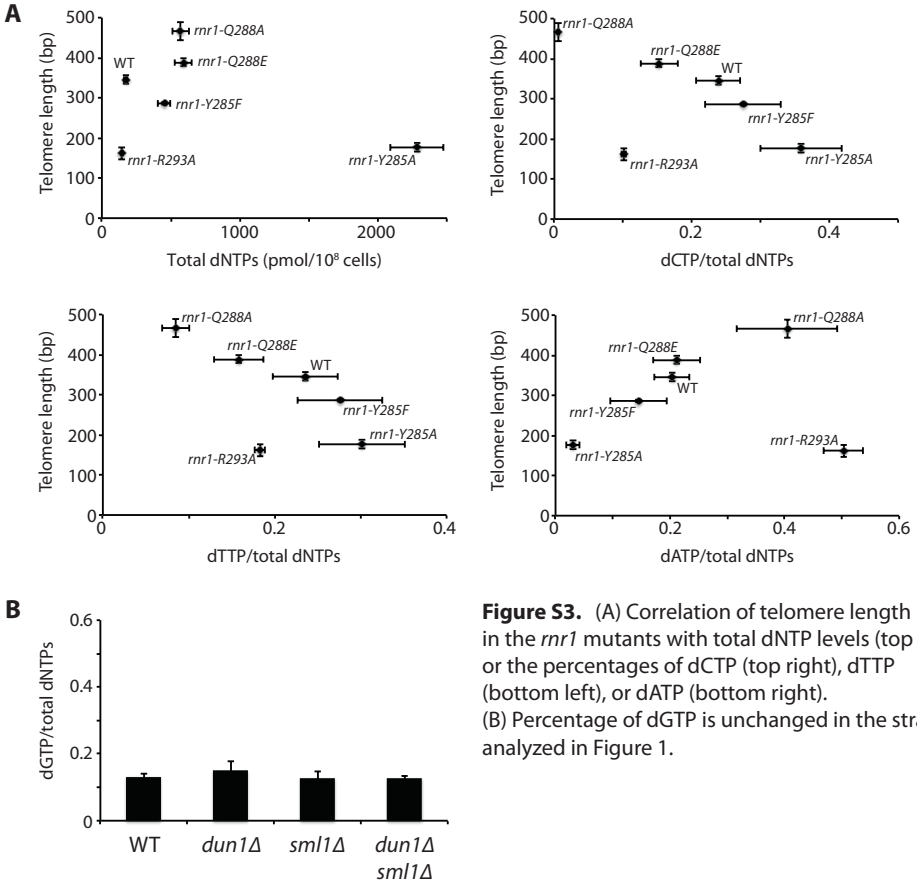

Figure S3. (A) Correlation of telomere length in the *rnr1* mutants with total dNTP levels (top left), or the percentages of dCTP (top right), dTTP (bottom left), or dATP (bottom right).
(B) Percentage of dGTP is unchanged in the strains analyzed in Figure 1.

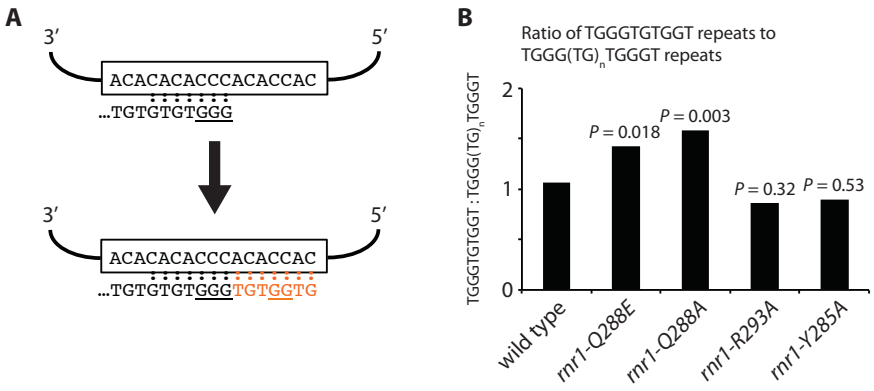

Figure S4. The processivity of reverse transcription of the 5′ portion of the TLC1 template region is increased in the *rnr1-Q288E* and *rnr1-Q288A* mutants. (A) Schematic illustrating the reverse transcription of the 5′ portion of the TLC1 template region, which is shown in the boxed area. Almost all telomeric repeats contain a GGG trinucleotide, but only about 50% of these repeats also contain the GG dinucleotide specified by the 5′ portion of the template region. (B) The ratio of GG-containing repeats (i.e. TGGGTGTGGT) to non-GG-containing repeats (i.e. TGGG(TG)$_n$TGGGT) is shown for a wild type strain and the four *rnr1* mutants. The *rnr1-Q288E* and *rnr1-Q288A* mutants, which have elongated telomeres, exhibit an increase in the presence of GG-containing repeats, indicating that telomerase repeat addition processivity for the 5′ portion of the TLC1 template region is increased. *P* values were determined using a chi-squared test to look whether the ratio in the mutant was significantly different from the wild type ratio.

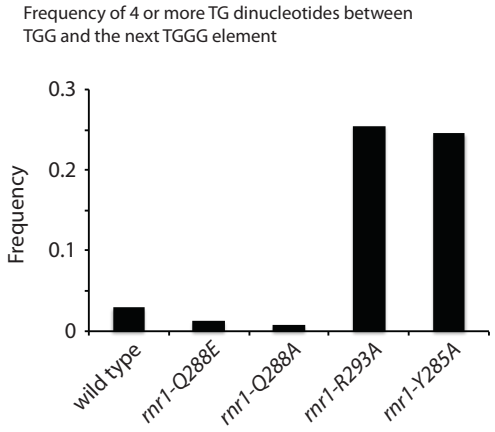

Figure S5. The frequency of having 4 or higher TG dinucleotides between a TGG and the following TGGG was plotted for the indicated strains.

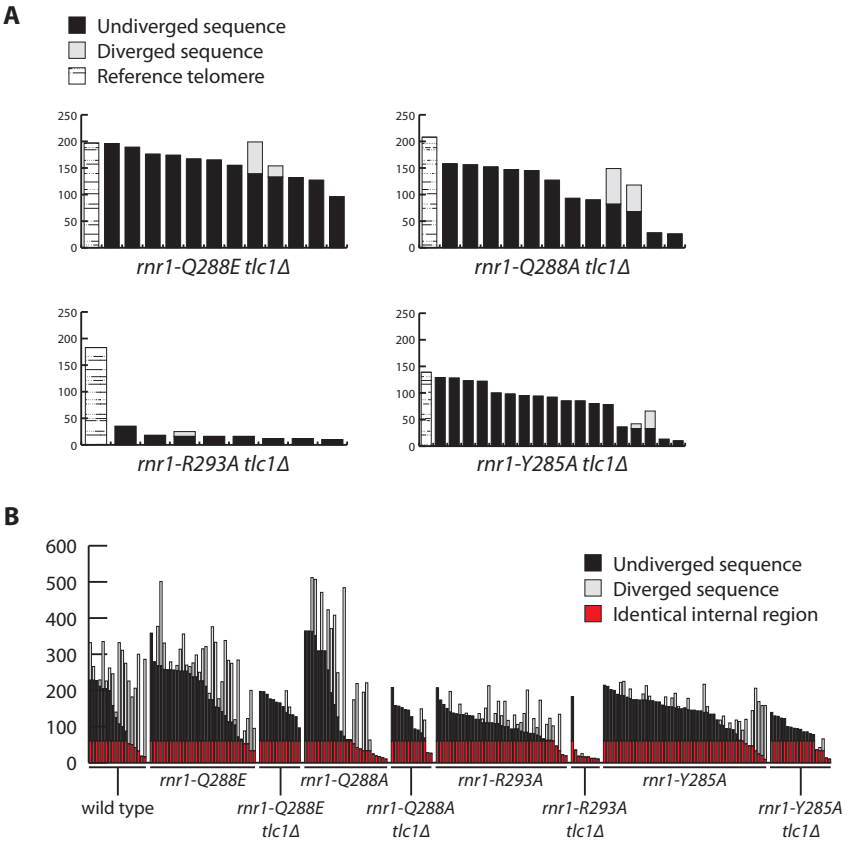

Figure S6. The telomere sequence changes in the *rnr1* mutants recorded in Figure 4 are telomerase-dependent. (A) Analysis of sequenced VI-R telomeres after ~30 generations of clonal expansion. Each bar represents an individual VI-R telomere and bars are sorted by the length of the undiverged sequence. The black portion of each bar represents the undiverged region of the telomere. The light gray portion represents the diverged region of the telomere. For each strain, the longest telomere without divergent sequence (hashed bar) is used as a reference telomere to which all other telomeres are compared to determine whether divergence has occurred. (B) All telomeres from all strains analyzed in this study share an identical internal region (as indicated by the red portion of each bars).

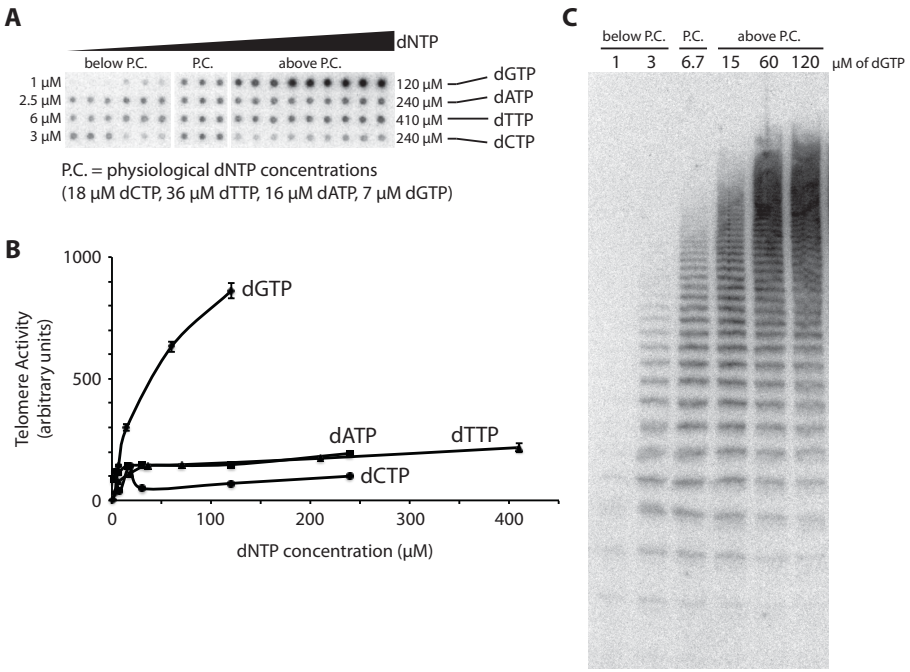

Figure S7. Human telomerase activity positively correlates with dGTP levels. (A) Telospot assay was performed by incubating crude "super-telomerase" extracts with a telomeric $(TTAGGG)_3$ primer and varying concentrations of dNTPs. "Physiological dNTP concentrations" used are derived from concentrations in yeast, although concentrations in mammalian cells are in the same range, as explained in the text. A small fraction of the reaction was directly spotted onto a nylon membrane, which is then probed with a randomly radiolabeled telomeric probe. Each reaction was spotted in triplicate. Each row of spots varies one of the four dNTPs, as indicated, from the lowest concentration shown on the left side to the highest concentration shown on the right. The reaction performed using physiological concentrations of all four dNTPs were spotted in triplicate, and then copy and pasted into each row for clarity. (B) Activity in each spot from A was quantified, and the mean for each reaction was plotted as a function of the concentration of the indicated dNTP. Error bars indicate the standard error. (C) The Telospot reactions with varying dGTP concentrations were repeated using a 5′-biotinylated $(TTAGGG)_3$ primer, purified with streptavidin-coated beads, resolved on a polyacrylamide gel, and transferred onto a nylon membrane. The membrane was then probed as in A. The concentration of dGTP used for each reaction is indicated above each lane.

TABLE S1 Yeast strains used in this study. All strains are derivatives of W1588-4C, except for BY4742, W9882 and the MCY strains. W9882 and the MCY strains are derivatives of BY4742.

Strain	Genotype	Reference
W1588-4C	*MAT***a** *ade2-1 can1-100 his3-11,15 leu2-3,112 trp1-1 ura3-1 RAD5*	(ZHAO *et al.* 1998)
W9557	*MAT***a**/α *dun1Δ::TRP1*/+ *sml1Δ::HIS3*/+	This study
W9875	*MAT***a**/α *dun1Δ::TRP1*/+ *sml1Δ::HIS3*/+ *crt1Δ::LEU2*/+	This study
W9877	*MAT***a**/α *dun1Δ::TRP1*/+ *tel1Δ::URA3*/+ *mec1-21*/+	This study
DK2A	*MAT*α *rnr1::[rnr1-R293A-URA3-pGAL-RNR1]*	(KUMAR *et al.* 2010)
DK2D	*MAT***a** *rnr1::[rnr1-R293A-URA3-pGAL-RNR1]*	(KUMAR *et al.* 2010)
DK8A	*MAT***a** *rnr1::[rnr1-Y285A-URA3-pGAL-RNR1]*	(KUMAR *et al.* 2010)
DK8E	*MAT*α *rnr1::[rnr1-Y285A-URA3-pGAL-RNR1]*	(KUMAR *et al.* 2010)
DK10E	*MAT***a** *rnr1::[rnr1-Q288A-URA3-pGAL-RNR1]*	(KUMAR *et al.* 2010)
JAK11-5B	*MAT*α *rnr1::[rnr1-Q288E-URA3-pGAL-RNR1]*	This study
JAK11-5C	*MAT***a** *rnr1::[rnr1-Q288E-URA3-pGAL-RNR1]*	This study
W9878	*MAT***a**/α *rnr1::[rnr1-Q288E-URA3-pGAL-RNR1]*/+ *tlc1Δ::HIS3*/+	This study
W9879	*MAT***a**/α *rnr1::[rnr1-Q288A-URA3-pGAL-RNR1]*/+ *tlc1Δ::HIS3*/+	This study
W9880	*MAT***a**/α *rnr1::[rnr1-R293A-URA3-pGAL-RNR1]*/+ *tlc1Δ::HIS3*/+	This study
W9881	*MAT***a**/α *rnr1::[rnr1-Y285A-URA3-pGAL RNR1]*/+ *tlc1Δ::HIS3*/+	This study
DK3A	*MAT***a** *rnr1::[rnr1-Y285F-URA3-pGAL RNR1]*	(KUMAR *et al.* 2010)
DK3C	*MAT***a** *rnr1::[rnr1-Y285F-URA3-pGAL RNR1]*	(KUMAR *et al.* 2010)
W4069-4C	*MAT***a** *RNR1 CAN1*	(CHABES *et al.* 2003)
W4069-8C	*MAT***a** *rnr1-D57N CAN1*	(CHABES *et al.* 2003)
W9100-12C	*MAT*α *ADE2*	This study
BY4742	*MAT*α *his3Δ1 leu2Δ0 lys2Δ0 ura3Δ0*	(BRACHMANN *et al.* 1998)
W9882	*MAT***a**/α *rnr1Δ::kanMX*/+	This study
MCY602	*MAT***a** *rnr1Δ::kanMX LYS2*	This study
MCY603	*MAT*α *rnr1Δ::kanMX*	This study
MCY605	*MAT*α *rnr3Δ::natMX*	This study
MCY606	*MAT*α *yil067cΔ::natMX*	This study
MCY607	*MAT*α *rnr1Δ::kanMX yil067cΔ::natMX*	This study

SUPPORTING REFERENCES

BRACHMANN, C. B., A. DAVIES, G. J. COST, E. CAPUTO, J. LI *et al.*, 1998 Designer deletion strains derived from *Saccharomyces cerevisiae* S288C: a useful set of strains and plasmids for PCR-mediated gene disruption and other applications. Yeast **14:** 115-132.

CHABES, A., B. GEORGIEVA, V. DOMKIN, X. ZHAO, R. ROTHSTEIN *et al.*, 2003 Survival of DNA damage in yeast directly depends on increased dNTP levels allowed by relaxed feedback inhibition of ribonucleotide reductase. Cell **112:** 391-401.

CRISTOFARI, G., P. REICHENBACH, P. O. REGAMEY, D. BANFI, M. CHAMBON *et al.*, 2007 Low- to high-throughput analysis of telomerase modulators with Telospot. Nat Methods **4:** 851-853.

DIONNE, I., and R. J. WELLINGER, 1996 Cell cycle-regulated generation of single-stranded G-rich DNA in the absence of telomerase. Proc Natl Acad Sci USA **93:** 13902-13907.

KUMAR, D., J. VIBERG, A. K. NILSSON and A. CHABES, 2010 Highly mutagenic and severely imbalanced dNTP pools can escape detection by the S-phase checkpoint. Nucleic Acids Res **38:** 3975-3983.

ZHAO, X., E. G. MULLER and R. ROTHSTEIN, 1998 A suppressor of two essential checkpoint genes identifies a novel protein that negatively affects dNTP pools. Mol Cell **2:** 329-340.